Significant Atmospheric CO2 Uptake by Antarctic Polynyas

Tae Rhee (rhee@kopri.re.kr)
Korea Polar Research Institute https://orcid.org/0000-0001-8025-9431
Christopher Zappa
Columbia University https://orcid.org/0000-0003-0041-2913
Young Kwon
Korea Institute of Ocean Science and Technology

Article

Keywords:

Posted Date: May 26th, 2022

DOI: https://doi.org/10.21203/rs.3.rs-1662382/v1

Significant Atmospheric CO_2 Uptake by Antarctic Polynyas

Tae Siek Rhee[1*], Christopher J. Zappa[2], and Young Shin Kwon[3]

[1]Korea Polar Ocean Research Institute, Incheon, Korea
[2]Lamont-Doherty Earth Observatory of Columbia University, Palisades, NY, USA
[3]Korea Institute of Ocean Science and Technology, Busan, Korea

*Corresponding author. e-mail: **rhee@kopri.re.kr**

Abstract: The Southern Ocean plays a pivotal role in controlling the most critical greenhouse gas, carbon dioxide (CO_2), in the atmosphere[1, 2]. However, insufficient observations, particularly in the Antarctic Sea Ice Zone (ASIZ; south of 60°S), hinders accurate estimation of the Southern Ocean sink strength of atmospheric CO_2[3, 4]. Here, we show that Antarctic polynyas play a significant role in the CO_2 budget of the Southern Ocean based on the 5-year continuous observations at the Korean Antarctic Station, Jang Bogo, in the Terra Nova Bay (TNB) polynya, Ross Sea, Antarctica and on the compilation of shipboard observations in the major Antarctic polynyas. The seasonal variation of the fugacity of dissolved CO_2 (fCO_2) between them shows in accordance, which was dominated by biological and physical processes in different seasons. Antarctic polynyas absorb atmospheric CO_2 at a rate of 9 to 14 Tg C a^{-1}, that is comparable to or more than the amount outgassed in the ASIZ, concentrating in the summer season from December to March. As the summer drawdown of fCO_2 in the polynya is dominantly driven by phytoplankton blooms which is in turn maintained by the supply of iron from circumpolar deep water and glacier melt water[5], we expect this CO_2 sink in the Antarctic polynyas to be enhanced in the future, resulting in a negative feedback with future climate change.

Approximately one quarter of the atmospheric CO_2 emitted by anthropogenic activities is taken up by the ocean, and one half of it takes place in the Southern Hemispheric oceans[3]. However, it is uncertain how significantly the Southern Ocean, south of 50°S, contributes to the atmospheric CO_2 variation since its sink strength varies widely from 0.05 to 0.6 Pg C a^{-1} [1, 3, 6, 7]. Various ocean and climate processes[8, 9] are attributed to these uncertainties, yet the low observation density among the ocean basins in spatial and temporal coverage hampers the accurate estimate and prediction of the role of the Southern Ocean in the atmospheric CO_2 cycle[3, 10]. The Southern Ocean exhibits added complexity in the CO_2 cycle because it is covered by a vast area of sea ice, which wanes and waxes seasonally. Recent intensified freshening by the decrease of sea ice extent enhances biological uptake of atmospheric CO_2 associated with strong and shoaling stratification of the surface mixed layer in the Western Antarctic Peninsula[11]. The Antarctic sea ice zone (ASIZ), the ocean surrounding Antarctica that includes varying degrees of sea ice, can be a source or sink of the atmospheric CO_2 depending on the season and sea ice concentration. Shipboard and float observations of the fugacity of dissolved CO_2 (fCO_2) in the surface ocean indicate emission of ~10 Tg C a^{-1} to the atmosphere[3, 12] in the ASIZ, while model calculation predicts a sink on an annual basis[4, 13].

Inside the ASIZ, katabatic winds traverse down the ice sheets, eventually blowing the sea ice away from the ice shelf edge to open the ocean to the atmosphere, forming polynyas surrounding Antarctica. Polynyas provide a unique conduit for heat and mass flux from the continental shelf ocean water since the water column is exposed to the atmosphere during the winter, and form dense water by brine rejection due to the formation of sea ice on the surface. The polynyas surrounding Antarctica produce source water that feeds the Antarctic Bottom Water (AABW)[14, 15]. Therefore, the material collected at the polynyas' air-sea interface is sequestered to

AABW for several hundreds to thousand years[16]. Sparse observations of dissolved seawater fCO_2 in the Antarctic polynyas show a drawdown of CO_2 in the summer driven by phytoplankton blooms that leads to uptake of atmospheric CO_2[17]. Lack of year-round observations, however, may bias the estimation of annual CO_2 flux in the Antarctic polynyas to that in summer season because even fewer observations exist in the fall, winter, and spring.

To bridge the seasonal gap of air-sea CO_2 flux in the Antarctic polynyas, we conducted continuous observations of fCO_2 in the air and the seawater in the Terra Nova Bay (TNB) polynya of the Ross Sea, Antarctica, since February, 2015 (Fig. 1) at the Korean Antarctic Station, Jang Bogo (JBG) (see Supplementary Information (SI) for details of method). Seawater was pumped to the automated fCO_2 analyzing system[18] installed in the laboratory onshore. In addition to dissolved CO_2, *in situ* seawater temperature and salinity and atmospheric CO_2 were monitored together. As the surface seawater circulates clockwise in TNB at a few tens of cm s^{-1} along the coast[19, 20], the fCO_2 observation at JBG likely represents the surface TNB fCO_2 since it occurs downstream of the surface waters of the TNB polynya. Sea ice concentration was estimated from the microwave data observed by AMSR-2 (seaice.uni-bremen.de) with the spatial resolution of 3.125×3.125 km^2 [21].

The dissolved fCO_2 in the TNB polynya seasonally varied from ~230 μatm to ~340 μatm, which is approximately one hundred times larger than the seasonal variation of atmospheric CO_2 concentrations (Fig. 2a). In early summer (December), the dissolved fCO_2 initially decreased rapidly with values ranging from 13 μatm d^{-1} for 10 days in 2016 to 40 μatm d^{-1} for 3 days in 2017. This sharp drawdown of dissolved fCO_2 did not immediately follow the sudden shrink of sea-ice concentration (Fig. 2a), but was delayed approximately from 10 days in 2017 to 40 days in 2015 and 2018. This is opposite to what has been presumed to be the impact of the sea-ice on the dissolved fCO_2 in the surface waters during polar spring associated with algae blooms, known as

74 the seasonal rectification hypothesis[22]. In addition, dilution of brine and dissolution of carbonate
75 precipitate in sea ice enhances the decrease of fCO_2 concentration during warming in the spring[23].
76 Our observation, however, does not support such vernal rectification processes of supersaturated
77 fCO_2 in the surface waters, but instead shows a continual increase of fCO_2 in spite of disappearing
78 sea ice. Therefore, we propose that the stratification of surface water driven by the combined effect
79 of radiative heating and freshening by melting of sea ice to be the prime precondition that initiates
80 the drop in the dissolved fCO_2 in the surface mixed layer in the TNB polynya. Historical
81 measurements of the profiles of temperature and salinity in the TNB polynya[24] suggests
82 stratification of the surface water starts developing in December with a very shallow mixed layer
83 depth in January, which is similar to the seasonal trend of the dissolved fCO_2 in the TNB polynya
84 but a month behind the beginning of the sea ice concentration decrease (Fig. S6). Mooring data of
85 temperature and salinity at 140 m deep in the TNB polynya also indicates deep convection of
86 surface seawater until December[24].

87 The decrease of dissolved fCO_2 continued until the late summer (the middle of February)
88 reaching the minimum daily values with the record low value of 93 μatm in 2016 and high value
89 of 211 μatm in 2018 (Fig. 2a), which coincide with maximum freshening in individual years (Fig.
90 2b). This suggests the stimulation of primary production by melting seawater or glacial melt water.
91 Abruptly, the dissolved fCO_2 increased rapidly with the onset of increase of the salinity and wind
92 speed that enhanced the uptake of atmospheric CO_2 (Fig. 2b, c) and deepening of the mixed layer
93 (Fig. S6), which in turn entrains the deep water containing high fCO_2. In the fall, the biological
94 production decreases precipitously leading to less CO_2 consumption, coupled with the continued
95 increase in wind speed, further increasing the uptake of atmospheric CO_2 and entrainment of deep
96 seawater. As the fall proceeds, sea ice production increases due to the high katabatic winds (Fig.

2a, c) and generates salty dense water, allowing vertical deep convection. This deep convection mixes water with high dissolved fCO_2 of ~440 μatm to the surface ocean that continues to increase above the equilibrium with respect to atmospheric CO_2, until reaching the deep water fCO_2 values. The increase of dissolved fCO_2 slowed down with the increase of the sea ice concentration in the TNB polynya.

Sea-to-air CO_2 flux in the TNB polynya was calculated by the product of the gas transfer velocity (k), the fCO_2 difference between the surface seawater and the overlying air (ΔfCO_2), and the CO_2 solubility at the temperature and salinity of the surface seawater[25] (See SI for details) (Fig. 2d). Apart from the case of fCO_2 itself in either the atmosphere or ocean, ΔfCO_2 variability is not relevant to the secular trend, but mostly to the physical, chemical and biological processes in the ocean. Therefore, it is not necessary to be normalized to a specific time. Since the solubility effect on the CO_2 flux is in general compensated by gas and momentum diffusivities in seawater[26], the range of variation of the sea surface temperature from -1.95 to 2.49°C and the salinity from 31.9 to 35.2 during the observation periods (Fig. 2b) influenced the CO_2 flux by merely 0.3% (1σ). The product of k and solubility termed the transfer coefficient, Tr (Fig. 2c), is therefore useful[3] as an indicator to the intensity of physical processes in gas exchange mostly driven by wind.

Wind speed generates upper-ocean turbulence that drives the gas transfer velocity and impacts the CO_2 flux directly. We adopted the Takahashi parameterization[3] for k that was determined on the basis of global budget of bomb ^{14}C and global mean wind speed, because it has been used to estimate global sea-to-air CO_2 flux including the ASIZ using shipborne observations. This parameterization, however, gives 50% less gas transfer velocity than the Wanninkhof quadratic parameterization[27], 10% larger than the Nightingale second-order polynomial parameterization[28] on average, both of which are often used to estimate CO_2 flux in the ocean.

Nonetheless, recent updated Wanninkhof parameterization[29] and direct determination of k in the ASIZ based on micrometeorological technique[30] are comparable to the Takahashi parameterization[3]. Here, we used the Wanninkhof[27] and Nightingale[28] parameterizations to estimate the maximal and minimal uncertainty of the flux. We use NCEP Reanalysis II data products[31] (NCEP2) as the representative wind field (Fig 2c) of the monthly mean neutral winds at 10 m high (U_{10N}) in addition to a comparison of several wind data products, *e.g.* NCEP1, JRA55, MERRA2, ERA5, and *in situ* shipboard and Automated Weather System observations at Manuela (MLA) on Inexpressible Island, located in the middle of the katabatic wind downhill from the Nansen ice shelf (see SI for details). The monthly mean U_{10N} of NCEP2 product reproduces the shipboard U_{10N} in TNB measured onboard the Korean Ice Breaker R/V Araon and is close to the *in situ* wind at MLA among the reanalysis wind products (Fig. S5). Furthermore, NCEP2 has been used to estimate global air-sea CO_2 exchange including the ASIZ[3], giving us the opportunity to compare the CO_2 flux directly without the potential bias due to the variability in wind speed among the wind products[32].

The impact of wind speed on CO_2 flux is demonstrated by comparing the monthly mean CO_2 fluxes in summer and early fall from January to March during the observation periods (Fig. 2d). Despite the low monthly mean magnitude of ΔfCO_2 (–140 to –89 μatm) in March every year that is almost half that in February (–255 to –167 μatm), the CO_2 flux in February (–20 to –13 g C m^{-2} month) and March (–20 to –12 g C m^{-2} month) are nearly equivalent because the wind speed is approximately 20% stronger in March. On the other hand, CO_2 monthly mean fluxes in January (–14 to –5 g C m^{-2} $month^{-1}$) are almost twice smaller than the values in February while the monthly mean magnitude of ΔfCO_2 (–209 to –126 μatm) in January is slightly (approximately 10 %) smaller. This is simply due to moderate wind speeds in January every year.

143 The relative contributions of ΔfCO_2, *Tr*, and polynya area to the CO_2 mass flow rate can be
144 visualized by the normalized monthly means with respect to that in February, the month that the
145 monthly CO_2 mass flow rate to the TNB polynya is largest (Fig. 3a). Here, we have introduced the
146 CO_2 mass flow rate, MFR, to distinguish the polynya area effects on the CO_2 flux and is defined
147 as the product of the CO_2 flux by polynya area, thus the unit of mass per time. The seasonal
148 variation of normalized MFR almost exactly follows that of the normalized ΔfCO_2 because its two
149 orders of magnitude difference between summer and winter overwhelms less than one order of
150 magnitude variation for *Tr* and polynya area (Fig. 3a), stressing the critical role of biological
151 activity in summer and vertical convection of the water column in winter in the TNB polynya.
152 However, during the wide open polynya period wind plays a significant role. MFR to the TNB
153 polynya was low in the early summer (December) due to the lowest *Tr*, showed strongest uptake
154 in the late summer (February) due to increased *Tr* and maximal magnitude of ΔfCO_2 and polynya
155 area, and returned to early summer values in the mid-fall (April) due to decreased magnitude of
156 ΔfCO_2 and polynya area even at high wind speeds. Early fall (March) exhibits the moderate
157 decrease in magnitude of both ΔfCO_2 and polynya area, but enhances MFR due to strong wind
158 approaching those in the winter, which in turn leads to the significant contribution of *Tr*. Thus, the
159 late summer (February) and early fall (March) are important contributors to carbon uptake by the
160 ocean in the TNB polynya. This is clearly demonstrated by the cumulative carbon content absorbed
161 by the TNB polynya (Fig. 3b). Even the steep accumulation of CO_2 emission in winter and spring
162 by the strong *in situ* wind at MLA was eventually compensated by the strong CO_2 uptake during
163 the late summer and early fall orchestrated by the high magnitude of ΔfCO_2, wide open polynya,
164 and considerable wind force in March.

165 In spite of the equivalent source (winter and spring) and sink (summer and fall) periods,

the total emission of CO_2 is merely 14% of total absorption on a yearly basis because of small polynya area and near CO_2 saturation. In fact, the sum of MFR in summer and early fall (January to March) is equivalent to the total annual carbon uptake (-113^{+7}_{-57} Gg C) emphasizing the importance of biological activity and large polynya area in summer in the CO_2 flux in the TNB polynya rather than strong wind in winter (Fig. 3b). Weighting the variation of the sea ice concentration in the TNB polynya, the annual CO_2 flux is estimated to be -31^{+1}_{-16} g C m^{-2} a^{-1}. This is more than 2-fold larger than any values observed in the polynyas and the continental shelves surrounding the Antarctic continent on annual basis[17, 33]. When applying wind data products other than NCEP2, the amount of annual carbon uptake is between –44 Gg C and –74 Gg C a^{-1} by ERA5, JRA55, MERRA2, and NCEP1 because their winds are biased to be weak year-round (Fig. S7). However, the strong *in situ* wind at MLA asserts annual uptake of atmospheric CO_2 by -99^{+30}_{-49} Gg C only, close to, although lesser than, the value estimated by NCEP2 on average.

Previous estimates of the CO_2 flux were made based on shipboard observations at random times during the annual cycle, often missing much of the important rapidly varying periods[17]. For the sake of the comparison of CO_2 flux in the TNB polynya, we also utilized shipboard observations compiled from both onboard Korean Ice Breaker R/V Araon and the Surface Ocean CO_2 Atlas (SOCAT) database version 2021[34] (Fig. 4). Accounting for the circulation time scale of a month for surface current[19, 20], we compared monthly mean values of observations at the JBG station to that for shipboard observation conducted in the same month in order to attest how representative the environmental parameters relevant to dissolved fCO_2 logged at JBG (see Fig. 2d). Analytical method and data treatment for dissolved CO_2 onboard R/V Araon is the same as that at JBG[18]. Areal normalization was applied by assigning the data points in the given grid of 0.25°×0.25° for a given month (e.g., see the pixel shown in the TNB polynya in Fig. 1). SOCAT

provides dry mole fraction of dissolved CO_2 (xCO_2), atmospheric pressure, sea surface temperature, and sea surface salinity, by which ΔfCO_2 can be derived. Among the months when both JBG and shipboard observations were conducted, all but February, 2018, and December, 2019, are within 3σ of the monthly variability of fCO_2 at JBG, and all months overlap each other within their variability (Fig. 2d and S5), suggesting that fCO_2 at JBG captures the variability of fCO_2 in the TNB polynya and supporting that JBG locates downstream of the clockwise circulation of TNB. Accounting for the rapid decrease in fCO_2 in early summer (December), the difference greater than 3σ in December, 2019, will not be unexpected. Comparison of sea surface temperature and salinity also strengthens the representativeness of the JBG observation as their difference in values between JBG and shipboard is within 3σ of *in situ* variability except in December, 2019, which again stresses the precipitous change in SST and SSS (Fig. 2b). For the case of calculating CO_2 flux using the shipboard and SOCAT data sets, we assume that the long record of the atmospheric CO_2 concentration at South Pole (www.esrl.noaa.gov/gmd/obop/spo) and NCEP2 reanalysis wind product are representative for the TNB polynya and the polynyas surrounding Antarctica as well.

Although the shipboard observations have been conducted occasionally for 20 years, they were concentrated in the summer and early fall from December to March (Fig. 4). During this season, 113^{+57}_{-7}Gg of atmospheric CO_2 was taken up by the TNB polynya on average (Fig 4d), which is merely 9% smaller on average than the estimate based on the continuous observation of fCO_2 at JBG for the same season. The small discrepancy comes mostly from the difference in fCO_2 as the monthly mean wind speeds and polynya areas are indifferent year to year (Fig. 4a).

Encouraged by the similarity in the annual MFR between the long-term JBG measurements and the SOCAT and R/V Araon spatial observations in the TNB polynya, we further explored MFR in the major polynyas surrounding Antarctica by the same approach as done to the TNB polynya

(Fig. 4). Polynyas in the Ross Sea, Amundsen Sea, Weddell Sea, Prydz bay, and Mertz bay were chosen as they account for ~75% of the polynya area surrounding Antarctica[35] (Fig. 1). The magnitude of mean ΔfCO_2 in the surface water is high in the summer and early fall (December to March) reaching -98 μatm, and significantly lower in winter and spring like the case of the TNB polynya measured at JBG (Fig. 4a). This suggests a low fCO_2 in the summer surrounding Antarctica to be a general feature driven by the marine primary production[35]. Due to fewer observations in seasons other than summer, it is hard to generalize seasonal variation of fCO_2 in the Antarctic polynyas. However, their similar features of seasonal variation to the TNB polynya allow us to use the current historic fCO_2 data to estimate the CO_2 flux and MFR in the polynyas surrounding Antarctica. Similar to TNB, the mean *Tr* varied throughout the year opposite to the magnitude of ΔfCO_2 (Fig. 4b). The polynya areas starts increasing in spring along with radiative heating, and reaches a maximum in late summer (Fig. 4c).

MFR in the major polynyas were calculated by multiplying monthly mean ΔfCO_2, *Tr*, and polynya area for the given polynyas (Fig. 4d). Polynya areas were derived from the microwave data observed by AMSR-E and AMSR-2[21] (seaice.uni-bremen.de). AMSR-E and AMSR-2 were not operational before 2002 and the transition period of the instruments in 2011 and 2012. Thus, we adopted the NSIDC data product[36] to complete the hiatus after adjusting the monthly mean sea ice concentrations to be consistent between them (see the method in SI). Lack of CO_2 flux in June and September due to no fCO_2 data in SOCAT was replaced by interpolation of the area-weighted mean flux of these major polynyas. The near saturation of the surface fCO_2 and small polynya area in winter and spring results in little impact to the annual MFR. Similar to the TNB polynya, the CO_2 flux in summer and early fall appears critical in the determination of annual MFR (Fig. 4d). Mean monthly MFR accelerated with time in summer due to an increase in polynya area and the

magnitude of ΔfCO_2 associated with intensifying primary production[35]. The total MFR in the major polynyas is estimated to be $-7^{+0.1}_{-3}$ Tg a^{-1} based on our calculation. Our estimate of the CO_2 uptake strength could be reduced to –3 to –4 Tg C a^{-1} using the wind products other than NCEP2 (Fig. 4d), which is unlikely in light of the comparison of various wind products described earlier. On the other hand, an extensive air-sea flux study in the Ross Sea[17] estimated the CO_2 sink as –7.5 Tg C a^{-1} using shipboard wind and Wanninkhof parameterization[27], the value approximately 30% larger than our estimate in the Ross Sea polynya. A modelling study argued much stronger uptake of atmospheric CO_2 in the Ross Sea polynya[37]. Accounting for the stronger shipboard wind than the reanalysis wind, the different fCO_2 database and sea ice concentration used, this would accord well with our estimate. Extending the major polynya areas to the entire polynyas surrounding Antarctica[35], the total MFR is increased to $-9^{+0.1}_{-5}$ Tg a^{-1}. Our estimate of the uptake strength of atmospheric CO_2 in the Antarctic polynyas is nearly equivalent to that in the south of 60°S surrounding Antarctica[3], but with opposite sign, implying that a significant contribution of the Antarctic polynyas in the Southern Ocean (*i.e.*, the uptake by the Antarctic polynyas is comparable to the outgassing by the Southern Ocean in the south of 60°S).

Primary production in the Southern Ocean is limited in spite of the sufficient amount of nutrients due to a deficiency in the amount of iron available. However, on the Antarctic continental shelf, a variety of sources of dissolved iron — the key micro-nutrient that triggers primary production in the Southern Ocean[38] — allows phytoplankton to thrive when sun light is available, leading to the enhancement of carbon fixation and atmospheric CO_2 uptake by the ocean. Melting ice sheets appear to be a primary source of the dissolved iron[5]. Recent acceleration of ice sheet retreat associated with positive trend of Southern Annular Mode[39], which forces the supply of the circumpolar deep water towards the Antarctic continental shelf, will elevate the supply of dissolved

iron. Together with the relatively long exposure to sun light, we expect the CO_2 sink in the Antarctic polynyas to be enhanced in the future, resulting in a negative feedback with future climate change.

References

1. Gruber N, Landschutzer P, Lovenduski NS. The Variable Southern Ocean Carbon Sink. *Annual Review of Marine Science* 2019, **11:** 159-186.

2. Sarmiento JL, Toggweiler JR. A new model for the role of the oceans in determining atmospheric P CO_2. *Nature* 1984, **308**(5960)**:** 621-624.

3. Takahashi T, Sutherland SC, Wanninkhof R, Sweeney C, Feely RA, Chipman DW*, et al.* Climatological mean and decadal change in surface ocean pCO_2, and net sea-air CO_2 flux over the global oceans. *Deep-Sea Research Part II-Topical Studies in Oceanography* 2009, **56**(8-10)**:** 554-577.

4. Gruber N, Gloor M, Fletcher SEM, Doney SC, Dutkiewicz S, Follows MJ*, et al.* Oceanic sources, sinks, and transport of atmospheric CO_2. *Global Biogeochemical Cycles* 2009, **23:** GB1005.

5. Arrigo KR, van Dijken GL, Strong AL. Environmental controls of marine productivity hot spots around Antarctica. *Journal of Geophysical Research-Oceans* 2015, **120**(8)**:** 5545-5565.

6. Takahashi T, Sutherland SC, Sweeney C, Poisson A, Metzl N, Tilbrook B*, et al.* Global sea-air CO_2 flux based on climatological surface ocean pCO_2, and seasonal biological and temperature effects. *Deep-Sea Research Part II-Topical Studies in Oceanography* 2002, **49**(9-10)**:** 1601-1622.

7. Long MC, Stephens BB, McKain K, Sweeney C, Keeling RF, Kort EA*, et al.* Strong Southern Ocean carbon uptake evident in airborne observations. *Science* 2021, **374**(6572)**:** 1275-1280.

8. DeVries T, Holzer M, Primeau F. Recent increase in oceanic carbon uptake driven by weaker upper-ocean overturning. *Nature* 2017, **542**(7640)**:** 215-218.

9. Landschutzer P, Gruber N, Haumann A, Rodenbeck C, Bakker DCE, van Heuven S*, et al.* The reinvigoration of the Southern Ocean carbon sink. *Science* 2015, **349**(6253)**:** 1221-1224.

10. Lenton A, Matear RJ, Tilbrook B. Design of an observational strategy for quantifying the Southern Ocean uptake of CO_2. *Global Biogeochemical Cycles* 2006, **20**(4)**:** GB4010.

11. Brown MS, Munro DR, Feehan CJ, Sweeney C, Ducklow HW, Schofield OM. Enhanced oceanic CO_2 uptake along the rapidly changing West Antarctic Peninsula. *Nature Climate Change* 2019, **9**(9)**:** 678-683.

12. Gray AR, Johnson KS, Bushinsky SM, Riser SC, Russell JL, Talley LD*, et al.* Autonomous Biogeochemical Floats Detect Significant Carbon Dioxide Outgassing in the High-Latitude Southern Ocean. *Geophysical Research Letters* 2018, **45**(17)**:** 9049-9057.

13. Lenton A, Tilbrook B, Law RM, Bakker D, Doney SC, Gruber N*, et al.* Sea-air CO_2 fluxes in the Southern Ocean for the period 1990-2009. *Biogeosciences* 2013, **10**(6)**:** 4037-4054.

14. Ohshima KI, Fukamachi Y, Williams GD, Nihashi S, Roquet F, Kitade Y*, et al.* Antarctic Bottom Water production by intense sea-ice formation in the Cape Darnley polynya. *Nature Geoscience* 2013, **6**(3)**:** 235-240.

15. Orsi AH, Johnson GC, Bullister JL. Circulation, mixing, and production of Antarctic Bottom Water. *Progress in Oceanography* 1999, **43:** 55-109.

16. England MH. The Age of Water and Ventilation Timescales in a Global Ocean Model. *Journal of Physical Oceanography* 1995, **25**(11)**:** 2756-2777.

17. DeJong HB, Dunbar RB. Air-Sea CO_2 Exchange in the Ross Sea, Antarctica. *Journal of Geophysical Research: Oceans* 2017, **122**(10)**:** 8167-8181.

18. Pierrot D, Neill C, Sullivan K, Castle R, Wanninkhof R, Luger H*, et al.* Recommendations for autonomous underway pCO_2 measuring systems and data-reduction routines. *Deep-Sea Research Part II-Topical Studies in Oceanography* 2009, **56**(8-10)**:** 512-522.

19. Picco P, Amici L, Meloni R, Langone L, Ravaioli M. Temporal variability of currents in the Ross Sea (Antarctica). In: Spezie G, Manzella GMR (eds). *Oceanography of the Ross Sea, Antarctica*. Springer: Milan, 1999, pp 103-117.

20. Flocco D, Falco P, Wadhams P, Spezie G. Surface current measurements in Terra Nova Bay by HF radar. *Antarctic Science* 2003, **15**(1)**:** 55-62.

21. Spreen G, Kaleschke L, Heygster G. Sea ice remote sensing using AMSR-E 89-GHz channels. *Journal of Geophysical Research: Oceans* 2008, **113**(C2)**:** C02S03.

22. Yager PL, Wallace DW, Johnson KM, Smith WO, Minnett PJ, Deming JW. The Northeast Water Polynya as an atmospheric CO_2 sink: A seasonal rectification hypothesis. *Journal of Geophysical Research: Oceans* 1995, **100**(C3)**:** 4389-4398.

23. Delille B, Vancoppenolle M, Geilfus NX, Tilbrook B, Lannuzel D, Schoemann V*, et al.* Southern Ocean CO_2 sink: The contribution of the sea ice. *Journal of Geophysical Research: Oceans* 2014, **119**(9)**:** 6340-6355.

24. Le Bel DA, Zappa CJ, Budillon G, Gordon AL. Salinity response to atmospheric forcing of the Terra Nova Bay polynya, Antarctica. *Antarctic Science* 2021, **33**(3)**:** 318-331.

25. Weiss RF. Carbon dioxide in water and seawater: the solubility of a non-ideal gas. *Marine Chemistry* 1974, **2:** 203-215.

26. Etcheto J, Merlivat L. Satellite determination of the carbon dioxide exchange coefficient at the ocean-atmosphere interface: A first step. *Journal of Geophysical Research: Oceans* 1988, **93**(C12)**:** 15669-15678.

27. Wanninkhof R. Relationship between wind speed and gas exchange over the ocean. *Journal of Geophysical Research* 1992, **97**(C5)**:** 7373-7382.

28. Nightingale PD, Malin G, Law CS, Watson AJ, Liss PS, Liddicoat MI*, et al.* In situ evaluation of air-sea gas exchange parameterizations using novel conservative and volatile tracers. *Global Biogeochemical Cycles* 2000, **14**(1)**:** 373-387.

29. Wanninkhof R. Relationship between wind speed and gas exchange over the ocean revisited. *Limnology and Oceanography: Methods* 2014, **12**(6)**:** 351-362.

30. Butterworth BJ, Miller SD. Air-sea exchange of carbon dioxide in the Southern Ocean and Antarctic marginal ice zone. *Geophysical Research Letters* 2016, **43**(13)**:** 7223-7230.

31. Kanamitsu M, Ebisuzaki W, Woollen J, Yang S-K, Hnilo J, Fiorino M*, et al.* NCEP–DOE AMIP-II reanalysis (R-2). *Bulletin of the American Meteorological Society* 2002, **83**(11)**:** 1631-1644.

32. Ramon J, Lledó L, Torralba V, Soret A, Doblas-Reyes FJ. What global reanalysis best represents near-surface winds? *Quarterly Journal of the Royal Meteorological Society* 2019, **145**(724)**:** 3236-3251.

33. Laruelle GG, Lauerwald R, Pfeil B, Regnier P. Regionalized global budget of the CO_2 exchange at the air-water interface in continental shelf seas. *Global biogeochemical cycles* 2014, **28**(11)**:** 1199-1214.

34. Bakker DCE, Pfeil B, Landa CS, Metzl N, O'Brien KM, Olsen A*, et al.* A multi-decade record of high-quality fCO_2 data in version 3 of the Surface Ocean CO_2 Atlas (SOCAT). *Earth System Science Data* 2016, **8**(2)**:** 383-413.

35. Arrigo KR, van Dijken GL. Phytoplankton dynamics within 37 Antarctic coastal polynya systems. *Journal of Geophysical Research-Oceans* 2003, **108**(C8)**:** 3271.

36. Comiso JC. Bootstrap Sea Ice Concentrations from Nimbus-7 SMMR and DMSP SSM/ISSMIS, Version 3.: NASA National Snow and Ice Data Center Distributed Active Archive Center; 2017. Report No.: NSIDC-0079.

37. Arrigo KR, van Dijken G, Long M. Coastal Southern Ocean: A strong anthropogenic CO2 sink. *Geophysical Research Letters* 2008, **35**(21).

38. Boyd PW, Jickells T, Law CS, Blain S, Boyle EA, Buesseler KO*, et al.* Mesoscale iron enrichment experiments 1993-2005: Synthesis and future directions. *Science* 2007, **315**(5812)**:** 612-617.

39. Rignot E, Jacobs SS. Rapid bottom melting widespread near Antarctic ice sheet grounding lines. *Science* 2002, **296**(5575)**:** 2020-2023.

Acknowledgements

We thank H.-G. Choi, J. H. Kim, and S. Kim for organizing the research programs, the overwintering engineers at the Korean Antarctic Station for caring for the pCO_2 analyzing instruments, and the SOCAT (Surface Ocean CO_2 Atlas) community and the University of Wisconsin-Madison Automatic Weather Station Program (NSF grant ANT-1543305) for the dataset. This work was supported by grants from the Korean Antarctic Polar Programs (PE22150 and PM22050), the National Research Foundation of Korea (NRF) grant funded by the Korean government (MSIT) (No. NRF-2018H1A2A1060886), and NSF Award Nos. ANT-0739519 and ANT-1341688 to Lamont-Doherty Earth Observatory of Columbia University. This is Lamont-Doherty Earth Observatory contribution number XXXX.

Contributions

T.S.R designed the study, T.S.R and C.J.Z. interpreted the data, T.S.R. and Y.S.K. collected the data, and all authors contribute to the preparation of the manuscript.

Competing interests

The authors declare no competing interests.

Code availability

All computing codes are available upon request.

Supplementary Information:

Supplementary Text

Figures

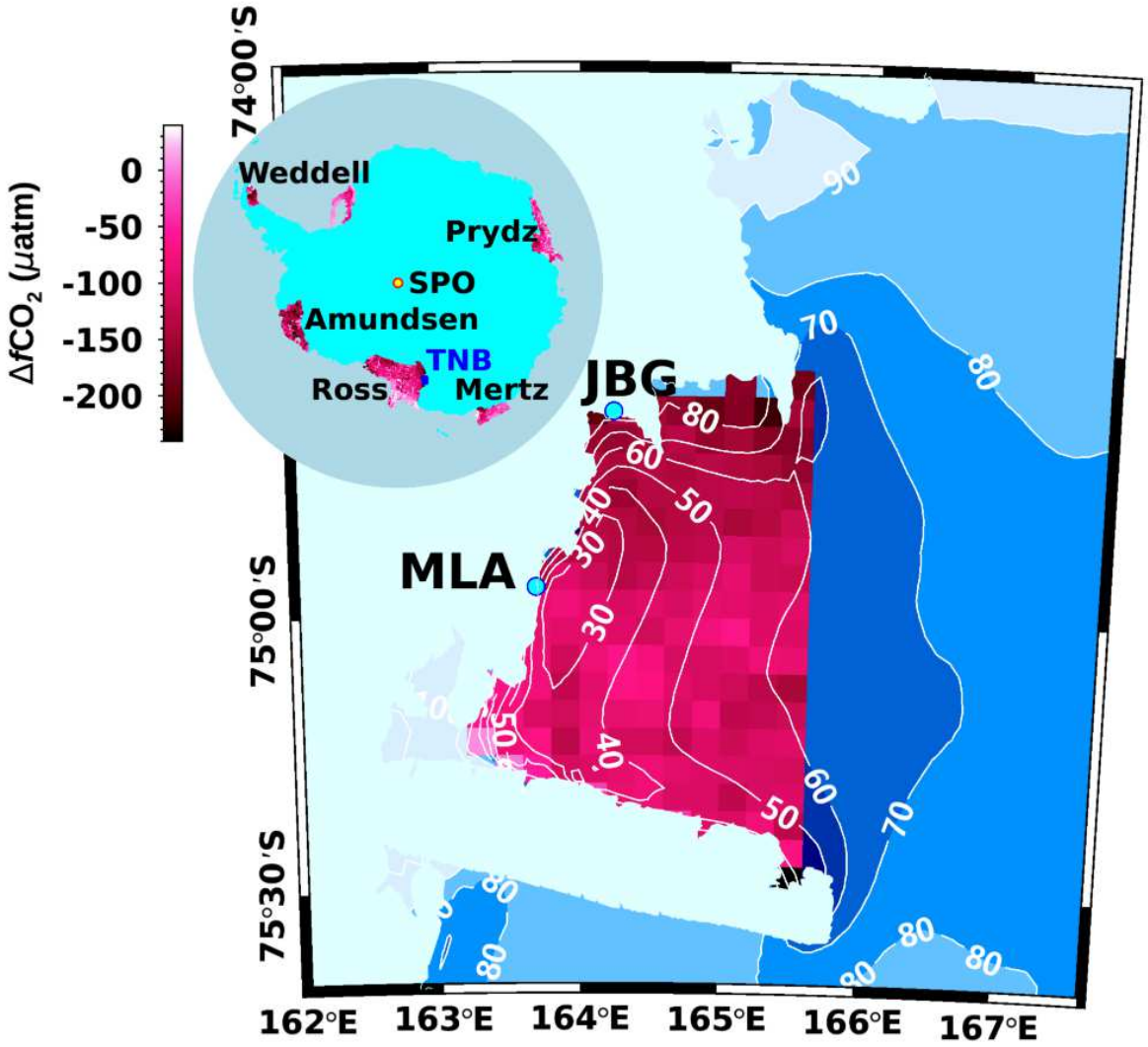

Fig. 1| Location of the Terra Nova Bay (TNB) polynya. Northern edge of the TNB polynya is bounded by the Jang Bogo (JBG) station allowing us to monitor the fCO_2 in the downstream surface waters. Blue tone with white contour lines in the TNB polynya indicates the 5-year mean sea ice concentrations in percentage from February 2015 to January 2020 that were estimated by the AMSR2 sea ice product from University of Bremen[21]. Inset represents major polynyas around Antarctica indicated by purple tone where its intensity translates the mean ΔfCO_2 in the given gird which was calculated using the SOCAT products version 2021[34]. The northern bound of the polynya was defined by the depth of 1000 m in bathymetry of the continental shelf[35]. The TNB polynya region defined in this study is also marked by the same scale of the purple tone as for the major polynyas in the map, and by the blue box in the inset. Wind speed measured at Manuela Automatic Weather Station (MLA) on Inexpressible Island, which is positioned at the center of katabatic wind, was used to define the representative wind data product over the TNB and major polynyas. Atmospheric CO_2 concentrations measured at the South Pole Observatory (SPO) run by NOAA air sampling network was assumed to be representative for the Antarctic polynyas.

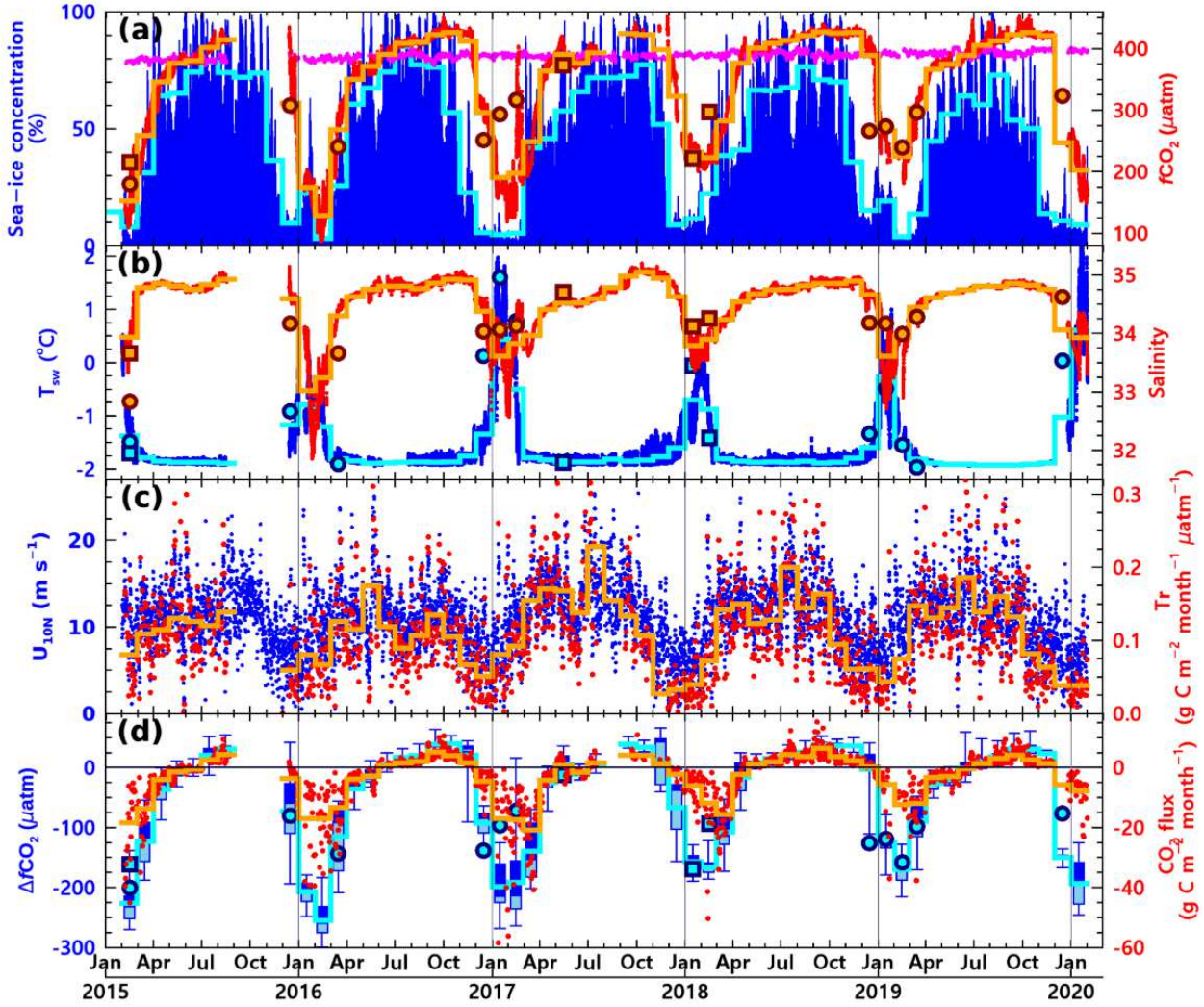

Fig. 2| 5-year observations of (a) atmospheric (pink) and ocean fCO_2 (red), and sea ice concentrations (blue), of (b) temperature (blue) and salinity (red), of (c) neutral wind speeds at 10 m above sea level (blue) and daily mean transfer coefficients, *Tr*, (red), and of (d) monthly box-whisker plot of ΔfCO_2 (blue) and of daily mean CO_2 flux (red) in the TNB polynya. Cyan- and orange-colored stepwise thick lines indicate monthly mean values for the blue and red parameters, respectively. Thick circle and square symbols represent monthly mean values for shipboard observations in the TNB polynya by R/V Araon and from the SOCAT products, respectively, and the symbol colors of cyan and orange corresponds to the blue and red parameters, respectively. In (d) the middle line of the box-whisker represents medium, the box for lower and upper quartiles, and the whisker for minimum and maximum values.

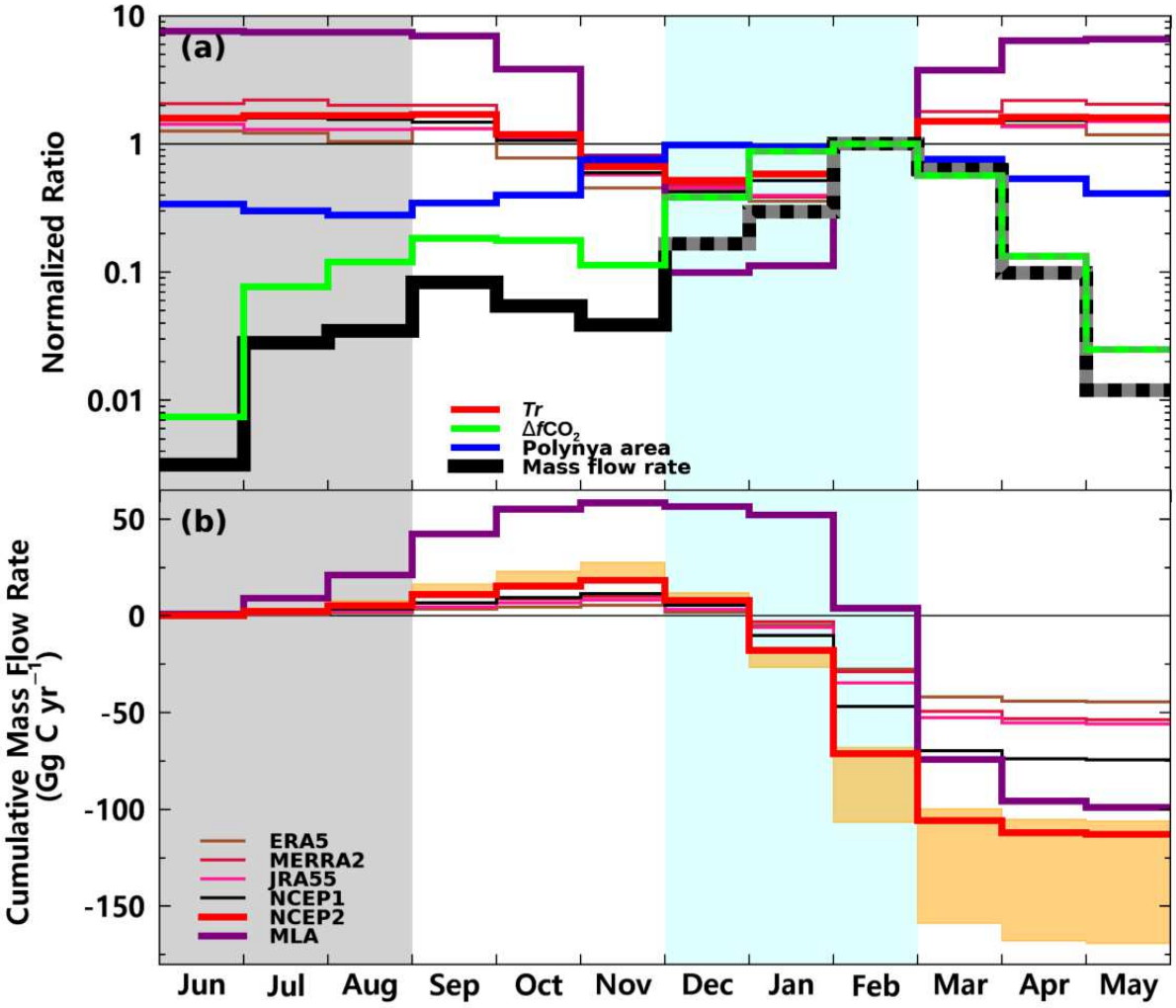

456 **Fig. 3|** (a) Monthly mean normalized ratio of the ΔfCO_2 (green), the transfer coefficient, *Tr* (red),
457 open water area in the TNB Polynya (blue) and the CO_2 mass flow rate, MFR, (black) and (b)
458 cumulative MFR (red) based on the 5-year observations. The normalized ratio is defined by
459 $\bar{X}/|\bar{X}_{avgFeb}|$, where $\bar{X}$ is the monthly mean and $|\bar{X}_{avgFeb}|$ is the absolute mean value for February.
460 Thin lines and red and purple thick lines in (a) and (b) refer to the various wind products indexed
461 in (b), which were fed into the calculation of *Tr* in (a) and the cumulative MFR using the Takahashi[3]
462 parameterization. For comparison, upper and lower bounds in orange shade in (b) indicate the
463 maximal and minimal magnitudes of MFR calculated by the Wanninkhof[27] and Nightingale[28]
464 parameterizations, respectively. The green-gray and black-gray stitched lines in (a) designate
465 negative sign with the absolute values assigned on the ordinate. Light gray and light cyan shades
466 in each panel indicate winter and summer, respectively.
467

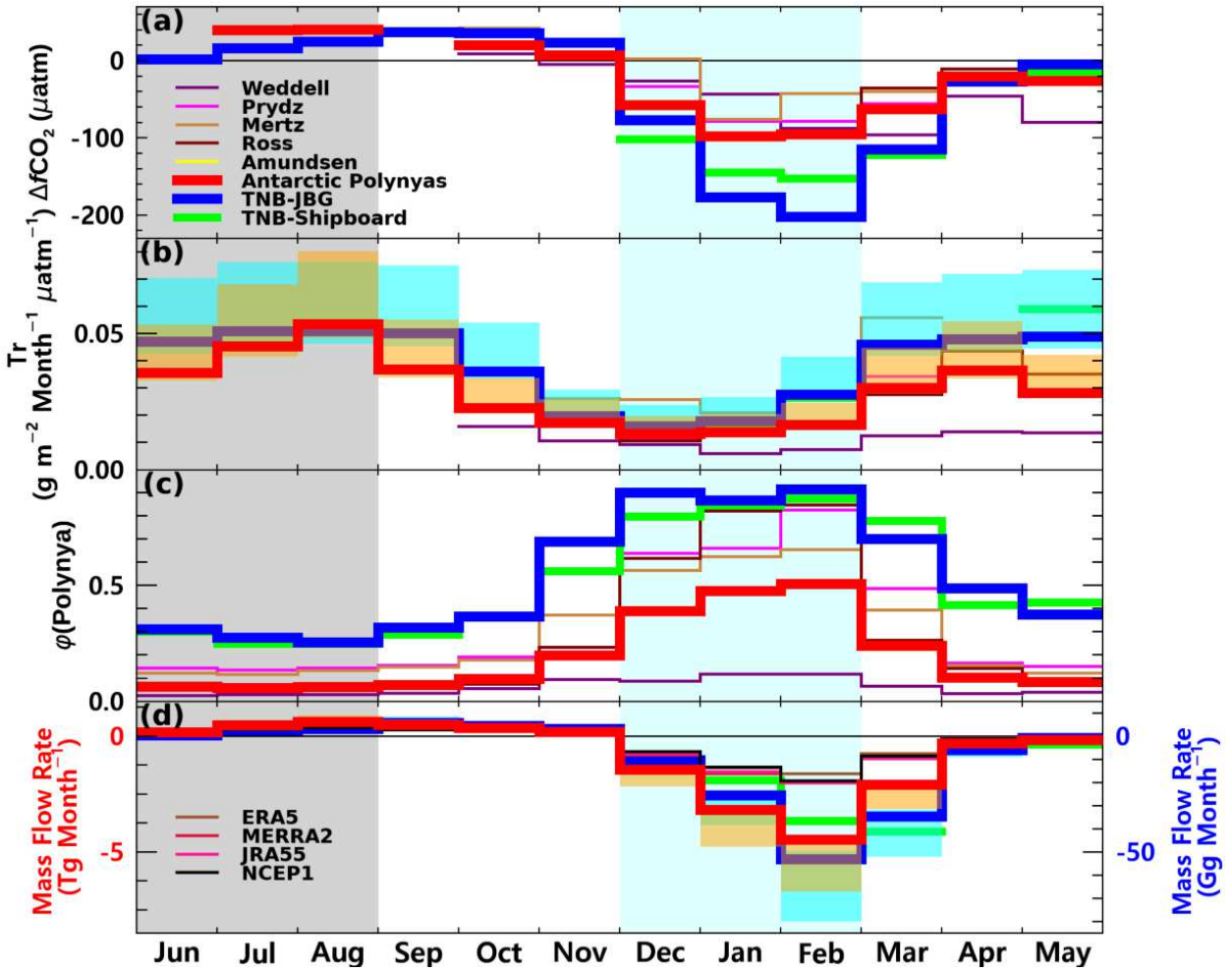

Fig. 4| Seasonal variations of (a) ΔfCO_2, (b) transfer coefficients, *Tr*, (c) polynya fractions, φ, and (d) the CO_2 mass flow rates, MFR, in the TNB polynya and the major polynyas. Thin lines with color codes in (a), (b), and (c) indicate the polynyas indexed in (a), and those in (d) are for the wind products applied to calculate MFR. Red thick line represents the mean values for the Antarctic polynyas, and blue and green for the TNB polynya based on JBG and shipboard observations, respectively. Orange and cyan shades in (b) and (d) indicate uncertainties calculated by the Wanninkhof[27] and Nightingale[28] parameterizations for maximum and minimum magnitudes, respectively. Note that units for MFR in (d) differ between the total Antarctic polynyas (red) and TNB polynya (blue and green). Light gray and light cyan shades indicate winter and summer season, respectively.

Supplementary Files

This is a list of supplementary files associated with this preprint. Click to download.

- Rheeetal2022PolynyaCO2FluxSI.pdf